Integrated optical modulator for signal up-conversion over radio-on-fiber link

Woo-Kyung Kim [1*], Soon-Woo Kwon [2], Woo-Jin Jeong [3], Geun-Sik Son [4], Kwang-Hyun Lee [5], Woo-Young Choi [5], Woo-Seok Yang [1], Hyung-Man Lee [1], and Han-Young Lee [1]

[1]*Korea Electronics Technology Institute, 68 Yatap-dong, Bundang-gu, Seongnam-si, Gyeonggi-do, Korea*
[2]*School of Advanced Materials Science and Engineering, Sungkyunkwan Univeristy, Gyeonggi-do, Korea*
[3]*Department of Electrical Engineering, University of Seoul,90 Jeonnong-dong, Dongdaemun-gu, Seoul, Korea*
[4]*Department of Electronic Engineering, Kwangwoon University, 447-1 Wolgye-dong, Nowon-gu, Seoul, Korea*
[5]*Department of Electrical and Electronic Engineering, Yonsei University, Seoul 120-749, Korea*
**Corresponding author: wkkim@keti.re.kr*

Abstract: An integrated optical modulator, which consists of a dual-sideband suppressed carrier (DSB-SC) modulator cascaded with a single-sideband (SSB) modulator, is proposed for signal up-conversion over Radio-on-Fiber. Utilizing a single-drive domain inverted structure in both modulators, balanced modulations were obtained without complicated radio frequency (RF) driving circuits and delicate RF phase adjustments. Intermediate frequency (IF) band signal was up-conversed to 60GHz band by using the fabricated device and was transmitted over optical fiber. Experiment results show that the proposed device enables millimeter wave generation and signal transmission without any power penalty caused by chromatic dispersion.

OCIS codes: (130.4110) Modulators; (130.3730) Lithium niobate; (130.3120) Integrated optics devices.

References and links

1. T. Kamisaka, T. Kuri, and K. Kitayama, " Simultaeous modulation and fiber-optic transmission of 10Gb/s baseband and 60GHz band radio signals on a single wavelength," IEEE Trans. Microwave Theory Tech. **49,** 2013-2017 (2001).
2. A. Martinez, V. Polo, and J. Marti, "Simultaneous baseband and RF optical modulation scheme for feeding wireless and wireline heterogeneous access network," IEEE Trans. Microwave Theory and Tech. **49,** 2018-2024 (2001).
3. X. Wang, N. J. Gomes, L. Gomez-Rojaz, P. A. Davies, and D. Wake, "Indirect optically injection-locked oscillator for millimeter-wave communication system," IEEE Trans. Microwave Theory and Tech. **48,** 2596-2603 (2000).
4. A. Martinez, V. Polo, H. Pfrommer, and J. Marti, "Dispersion-tolerant transmission of QPSK and M-QAM signals simultaneously modulated at 1 and 38GHz over a hybrid fiber-radio link," IEEE Photon. Tech. Lett. **16**, 659-661 (2004).
5. H. Furuta, M. Maeda, T. Nomoto, J. Kobayashi, and S. Kawasaki, "Optical Injection Locking of a 38-GHz-Band InP-Based HEMT Oscillator Using a 1.55-μm DSB-SC Modulated Lightwave," IEEE Microwave Wireless Components Lett. **11**, 19-21 (2001).
6. F. Lucchi, D. Janner, M. Belmonte, S. Balsamo, M. Villa, S. Giurgiola, P. Vergani, and V. Pruneri., "Very low voltage single drive domain inverted $LiNbO_3$ integrated electro-optic modulator," Opt. Express **15**, 10739-10743 (2007).
7. W.-K. Kim, W.-J. Jeong, S.-W. Kwon, M.-K. Song, G.-S. Son, W.-S. Yang, H.-M. Lee, and H.-Y. Lee, "60GHz optical carrier generation using a domain reversed $LiNbO_3$ optical modulator," J. Lightwave Technol. **26**, 2269-2273 (2008).
8. R. C. Alferness, S. K. Korotky, and E. A. J. Marcatili, "Velocity-matching techniques for integrated optic traveling wave switch/modulators," IEEE J. Quantum Electron **QE-20**, 301-309 (1984).
9. W. Wang, R. Tavlykaev, and R. V. Ramaswamy, "Bandpass traveling-wave Mach-Zehnder modulator in $LiNbO_3$ with Domain Reversal," IEEE Photon. Technol. Lett. **9**, 610-612 (1997).
10. G. H. Smith, D. Novak, and Z. Ahmed, "Technique for optical SSB generation to overcome dispersion penalties in fibre-radio systems," Electron. Lett. **22**, 74-75 (1997).
11. R. A. Griffin, P. M. Lane, and J. J. O'Reilly, "Dispersion-tolerant subcarrier data modulation of optical millimeter-wave signals," Electron. Lett. **32**, 2258-2260 (1999).

#101333 - $15.00 USD Received 8 Sep 2008; revised 16 Jan 2009; accepted 21 Jan 2009; published 9 Feb 2009

12. J. Yu, G. C. Kung, H. Muhammad, and J. Barry, "10 Gbit/s repeaterless transmission over 265 km SMF-28: using a modified duo-binary RZ signal generated by one dual-drive $LiNbO_3$ modulator," Opt. Commun. **239**, 99-101 (2004).

1. Introduction

Millimeter wave (MMW) communication has attracted attention because a demand for increased data capacity has grown with a ubiquitous wireless technology. But MMW generation and transmission is faced with serious problems such as high cost and great loss in a conventional coaxial cable. Therefore radio-on-fiber (RoF) becomes a promising technology for MMW wireless communication [1-2].

MMW generations are key techniques in RoF systems and there are several approaches. MMW optical carrier using a mode-locked or two phase-locked laer sources was proposed [3]. However, it is difficult to maintain the constant optical phase difference between the two spectrum components, since phase lock conditions are sensitive to mechanical vibration, temperature change, electric noise, etc. The optical MMW generations using an external Mach-Zehnder modulator (MZM) based on dual-sideband suppressed carrier (DSB-SC), have been demonstrated [4-5]. However, these image rejection architectures need balanced modulation such as in dual electrode MZM.

For efficient MMW up-conversion, we propose the integrated optical modulator, which consists of a DSB-SC modulator cascaded with an SSB modulator. 60GHz MMW optical carrier is generated by the first MZM, and intermediate frequency (IF) band SSB modulation is performed by the second one to overcome the power penalty due to chromatic dispersion effects. Utilizing a single-drive domain inverted structure in both modulators, balanced modulations are obtained without complicated RF driving circuits and delicate RF phase adjustments. Designs and fabrications for a proposed integrated modulator are present in this paper. IF band signal was up-conversed to 60GHz band by using the fabricated device and was transmitted over optical fiber. Measuring the up-converted RF power fluctuation as a function with transmitted length, we also investigated the power penalty caused by fiber chromatic dispersion.

2. Operation principle

2.1 Device structure and function.

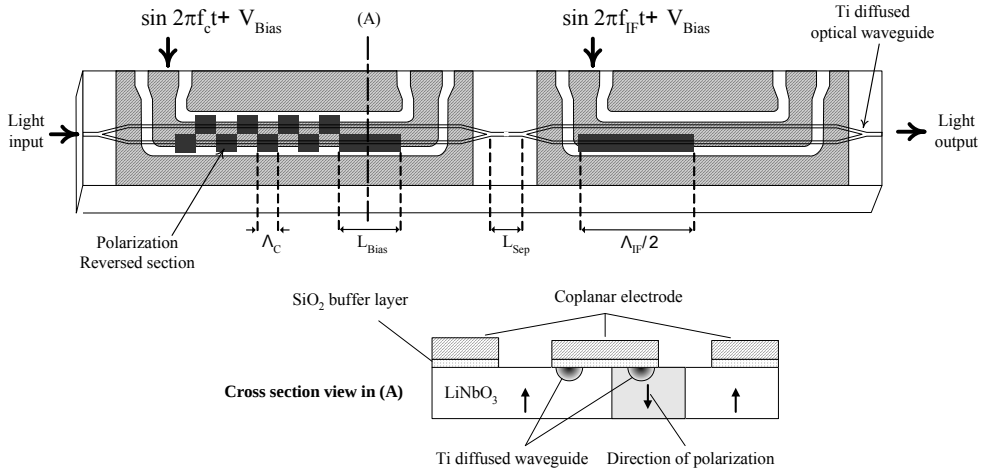

Fig. 1. A schematic of the integrated modulator with polarization reversed structures.

Figure 1 shows the schematic of the proposed integrated optical modulator for 60GHz RoF application. The integrated modulator consists of the DSB-SC modulator and the IF band SSB modulator. Two Mach-Zehnder Interferometers (MZI) are formed in series by using Ti

#101333 - $15.00 USD Received 8 Sep 2008; revised 16 Jan 2009; accepted 21 Jan 2009; published 9 Feb 2009

diffusion into a z-cut $LiNbO_3$ substrate. Wide hot-electrodes in both modulators, is located on MZI for the balanced modulation [6-7]. In the DSB-SC modulator, two periodically polarization reversed structure for the quasi-velocity-matching (QVM) are formed along two straight waveguides of the MZI [7-9]. The period of polarization reversal, $2\Lambda_c$, can be obtained from the calculated effective index of RF [8]. The polarization reversal periods are same in the two waveguides; however, their domains are polarized in the opposite orientation. In addition, for DC bias operation, a nonperiodic polarization-reversed region is placed at the end of the interaction region. The length of the nonperiodic region is adjusted to the polarization period, $2\Lambda_c$. Therefore, millimeter-wave modulation characteristics are not affected.

In the SSB modulator, a local region with the length of $\Lambda_{IF}/2$ is domain inverted. A interaction length of a IF band SSB modulator is Λ_{IF}, which can be calculated from the phase velocity difference between IF signal and optic. This structure enables only SSB modulation but the bias operation by DC. (A detail discussion about SSB modulation scheme is placed in Section *2.2*)

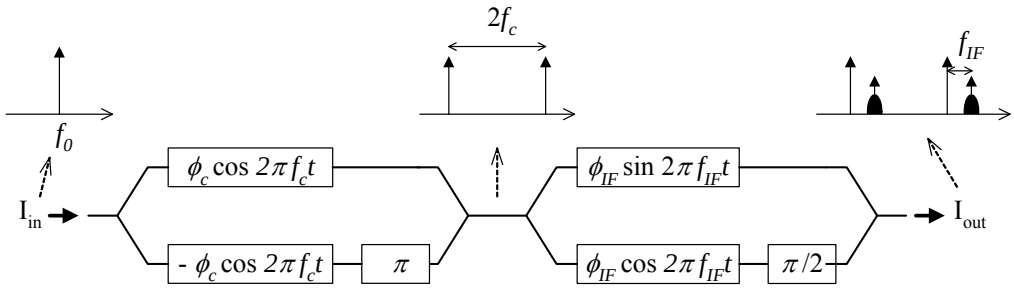

Fig. 2. Block diagram and modulated optical spectra.

Modulation in the integrated modulator, as shown in Fig. 1, can be expressed by functional elements as shown in Fig. 2. Applying a modulating frequency of f_c to the first electrode, the phases of optical signal in two waveguides are modulated with the modulation index of ϕ_c, but the signs of modulated phases are opposite due to a complementary polarization reversed structure as shown in Fig. 1. When the phase difference between two waveguides of MZI is kept at π by applying DC bias, DSB-SC modulation is performed and the output of the first MZI has sub-carriers $f_0 + f_c$ and $f_0 - f_c$ as shown in Fig. 2. Adding IF band frequency, f_{IF}, to the second MZI and adjusting the optical phase difference between two waveguides to $\pi/2$, we can get a SSB modulated signal with the modulation index of ϕ_{IF}. And the output of the second MZI has additional upper side band (USB) signals at $(f_0 + f_c) + f_{IF}$ and $(f_0 - f_c) + f_{IF}$. Modulated optical signals are sent via the fiber-optic distribution network to the remote antenna units where optical heterodyning in a wide bandwidth photodiode takes place, and the MW at $2f_c - f_{IF}$ and $2f_c + f_{IF}$ can be generated.

2.2 SSB Modulation using locally domain-inverted structure

Since a functional modulator using periodic domain inversion has band pass characteristics, a separate electrode for the DC Bias is needed. And it makes integration of modulator difficult. However, locally domain-inverted structure can enable the control of the optical phase delay by DC bias.

#101333 - $15.00 USD Received 8 Sep 2008; revised 16 Jan 2009; accepted 21 Jan 2009; published 9 Feb 2009

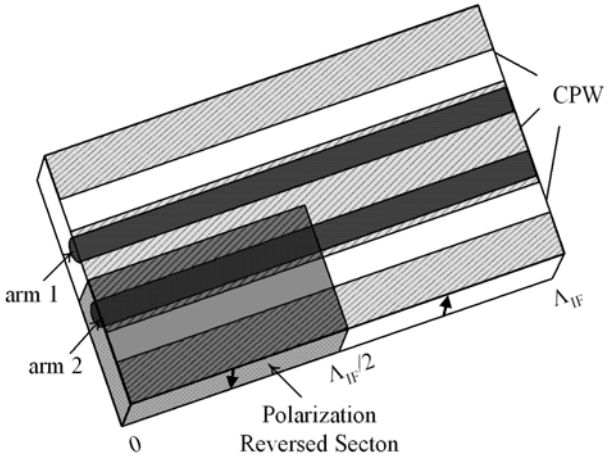

Fig. 3. Interaction region of a SSB modulator with locally domain-inverted structure.

Figure 3 describes the interaction region in the IF band SSB optical modulator, with a locally domain inverted structure. The electric field $E_0(t,z)$ of optic and modulating voltage $V(t,z)$ is expressed respectively as follows:

$$E_0(t,z) = e^{j\left(2\pi f_0\left(t-\frac{n_0}{c}\right)z\right)} \tag{1}$$

$$V(t,z) = Ae^{-\alpha_{IF}z}\sin\left(2\pi f_{IF}\left(t-\frac{n_{IF}}{c}z\right)\right) \tag{2}$$

α_{IF} and n_{IF} denotes the attenuation constant and the effective index of MW respectively. n_0 also denotes the effective index of optic.

Integrated effective voltages on the arm 1 and the arm 2, V_{eff1} and V_{eff2}, are

$$\begin{aligned} V_{eff1} &= \int_0^{\Lambda_{IF}} V\left(t+\frac{n_0}{c}z,z\right)dz \\ &= \frac{A}{\alpha_{IF}^2+k^2}\left[\alpha_{IF}\cdot\left(1+e^{-\alpha_{IF}\Lambda_{IF}}\right)\sin\left(2\pi f_{IF}t\right)-k\cdot\left(1+e^{-\alpha_{IF}\Lambda_{IF}}\right)\cos\left(2\pi f_{IF}t\right)\right] \end{aligned} \tag{3}$$

$$\begin{aligned} V_{eff2} &= -\int_0^{\frac{\Lambda_{IF}}{2}} V\left(t+\frac{n_0}{c}z,z\right)dz + \int_{\frac{\Lambda_{IF}}{2}}^{\Lambda_{IF}} V\left(t+\frac{n_0}{c}z,z\right)dz \\ &= \frac{A}{\alpha_{IF}^2+k^2}\left[\left(k-k\cdot e^{-\alpha_{IF}\Lambda_{IF}}-2\alpha_{IF}\cdot e^{-\alpha_{IF}\frac{\Lambda_{IF}}{2}}\right)\cos\left(2\pi f_{IF}t\right)\right. \\ &\qquad \left.-\left(2k\cdot e^{-\alpha_{IF}\frac{\Lambda_{IF}}{2}}+\alpha_{IF}-\alpha_{IF}\cdot e^{-\alpha_{IF}\Lambda_{IF}}\right)\sin\left(2\pi f_{IF}t\right)\right] \end{aligned} \tag{4}$$

,where $\Lambda_{IF} = \frac{c}{2f_{IF}(n_{IF}-n_0)}$, $k = \frac{\pi}{\Lambda_{IF}}$, c :light velocity in vacuum (5)

#101333 - $15.00 USD Received 8 Sep 2008; revised 16 Jan 2009; accepted 21 Jan 2009; published 9 Feb 2009

By supposing that MW waveguide is lossless, we can obtain the expressions of V_{eff1} and V_{eff2} in simple forms.

$$V_{eff1} = -\frac{2A}{k}\cos\left(2\pi f_{IF} t\right) \tag{6}$$

$$V_{eff2} = -\frac{2A}{k}\sin\left(2\pi f_{IF} t\right) \tag{7}$$

Equations (6) and (7) reveal that two effective voltages with $\pi/2$ phase difference can be obtained using a locally domain-inverted structure as shown in Fig. 3 and enable SSB modulation.

3. Experiment and characterization

We first fabricated the two MZIs with single-mode channel waveguides on a 0.5 mm thick 3 inch z-cut $LiNbO_3$ wafer using a titanium thermal diffusion method. 95 nm thick, 7 μm wide Ti strips were formed on the –z surface of the $LiNbO_3$, and the sample was heated to 1060 ℃ in a furnace with an argon atmosphere for 8 hours. To prevent the deterioration in extinction ratio due to directional coupling between two arms of the MZI, the separation of the MZI was set to 20 μm. After fabricating the Ti-diffused waveguides, we polished the +z surface of the $LiNbO_3$ wafer to remove a spontaneous domain-reversed layer, which was created during the diffusion process. Next, the polarization in a selective area was reversed by an electric field poling method [7]. The substrate was then coated with a buffer layer of silicon dioxide. A coplanar waveguide (CPW) composed of gold electrode was employed to provide a good connection to an external circuit. The characteristic impedance of 35 Ω was achieved from CPW parameters as listed in Table 1.

Table 1. Parameters of the fabricated modulator

Ti stripe width	7 μm
The gap between the two waveguides in MZI	20 μm
The separation of two MZI, L_{sep}	10 mm
Hot electrode width	38 μm
Electrode spacing	50 μm
Electrode thickness	6 μm
SiO2 buffer layer thickness	0.4 μm
Period of polarization reversal in DSB-SC modulator, $2\Lambda_c$	6.2 mm
Number of periods	4
The length of non-periodic region for DC bias, L_{Bias}	6.2 mm
Interaction length in SSB modulator, Λ_{IF}	16.9 mm

The fabricated device was pigtailed to a polarization maintain fiber for input and a single mode fiber for output, both of which have 8 degree end-polished faces. The fiber-to-fiber optical insertion loss measured was 7.3 dB. The fabricated modulator was RF-packaged with a V-connector and 50 Ω termination. The measured DC switching voltage, Vπ, of DSB-SC and SSB modulator were 16V and 11.7V, respectively. And the calculated Vπ·L products was about 10V·cm.

#101333 - $15.00 USD Received 8 Sep 2008; revised 16 Jan 2009; accepted 21 Jan 2009; published 9 Feb 2009

A 60GHz optical carrier was generated by using the DSB-SC modulation scheme, and simultaneously a SSB modulation was performed for up-conversion of IF signal to MMW. A sinusoidal microwave signal, with a 30 GHz modulation frequency and 20 dBm RF power, was applied to the first modulator by adjusting the DC bias voltage to the minimum point of optical power. For SSB modulation, 5.5 GHz IF signal with 18dBm RF power was applied to the second modulator.

Figure 4 shows the modulated spectra of output signals. The un-modulated spectrum, which depicted by hollow circles, are drawn as well for comparison's purpose. From the figure, we confirm that the modulated optical signal contains two sub-carriers with a 60GHz interval and IF signal is placed only on the left (or right) hand to the sub-carrier. The optical phase delay in SSB modulator could be regulated by DC bias voltage. For example, the suppressed optical sideband was distinctively switched from the upper sideband to the lower sideband by changing the DC bias voltage from 1.9V to -10.6V. We also measured a beat signal of the modulated output, by feeding the optical signal as shown in Fig. 4 to a high-speed photodetector and the results are shown in Fig. 5. Figures reveal that IF signal can be successfully up-conversed to MMW (about 54.5GHz or 65.5GHz) by using the proposed device.

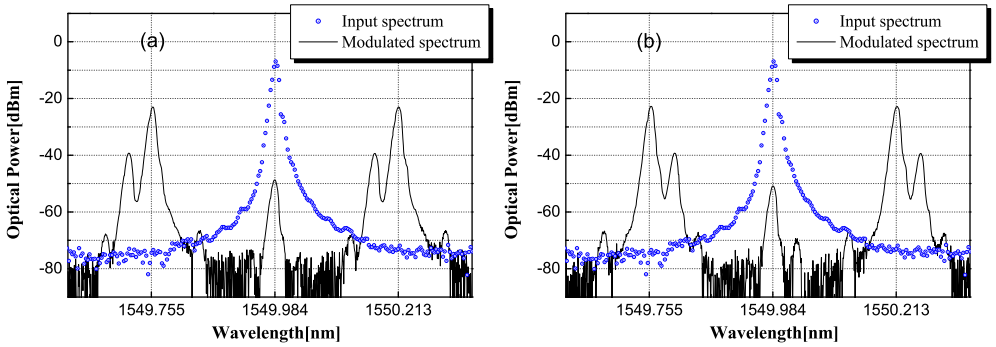

Fig. 4. Measured optical frequency spectra from the fabricated integrated modulator. The DC bias voltage in SSB modulator was 1.9 V for (a), and -10.6 V for (b).

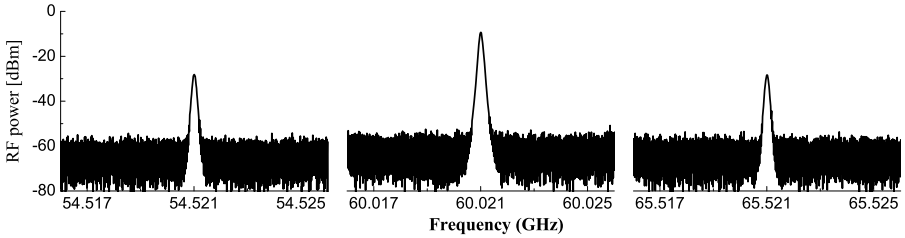

Fig. 5. RF spectra generated from modulated optical signal as shown in Fig. 4.

4. Chromatic dispersion effects dependence on modulation scheme

Figure 6 shows the experiment setup for investigating the effects of fiber chromatic dispersion. A 60GHz optical carrier was generated by applying 31.5GHz source with 20dBm RF power to the DSB-SC modulator. And then 5.5GHz IF source was applied to the second modulator while DSB or SSB modulation was performed by changing the DC bias voltage. The modulated signal was transmitted over standard single-mode fiber with different length from 0 to 40km. To eliminate the fiber loss effect due to different transmission distances, a variable optical attenuator (VOA) was engaged. The effects of dispersion were investigated by measuring the RF power recovered at USB (68.5GHz) or LSB (57.5GHz).

#101333 - $15.00 USD Received 8 Sep 2008; revised 16 Jan 2009; accepted 21 Jan 2009; published 9 Feb 2009

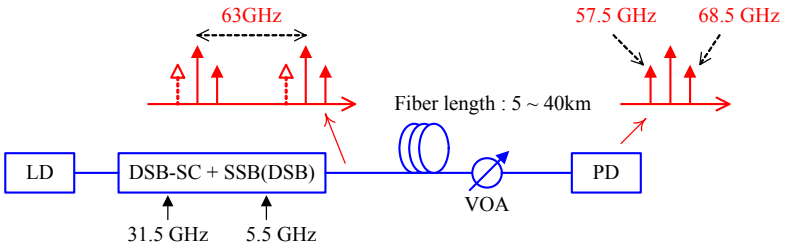

Fig. 6. Experiment setup for investigating the effects of fiber chromatic dispersion.

Figure 7 shows the measured RF power penalty of transmitted signal using the DSB modulation. Figures reveal that large power degradations was repeatedly observed at certain transmission distances and the degradation period for USB (68.5GHz) is shorter than that for LSB (57.5GHz). These power penalties are due to chromatic dispersion, which causes each spectral component to experience different phase shifts depending on the fiber link distance, modulation frequency, and the fiber dispersion parameter [10]. The experiment results agree reasonably with the calculated from an equation below [11], where dispersion of SMF-28, D was set to 17 ps/nm/km [12].

$$P_{LSB} \propto \cos^2\left[\pi\left(2 f_c f_{IF} - f_{IF}^2\right)\lambda^2 DL/c\right] + \varphi \tag{8}$$

$$P_{USB} \propto \cos^2\left[\pi\left(2 f_c f_{IF} + f_{IF}^2\right)\lambda^2 DL/c\right] + \varphi, \tag{9}$$

where c :light velocity in air, L : transmitted distance.

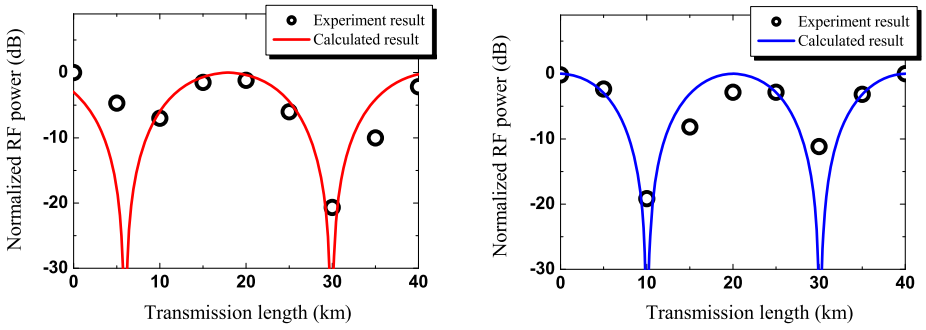

(a) LSB (57.5GHz) (b) USB (68.5GHz)

Fig. 7. Measured RF power penalties for optical DSB modulation versus transmittance length.

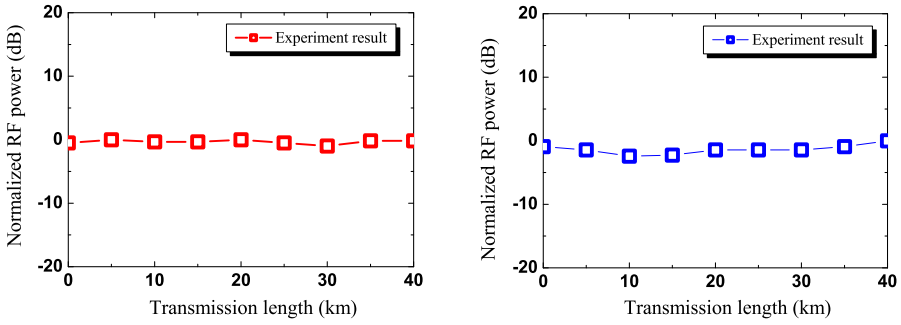

(a) LSB (57.5GHz) (b) USB (68.5GHz)

Fig. 8. Measured RF power penalties for optical SSB modulation versus transmittance length.

#101333 - $15.00 USD Received 8 Sep 2008; revised 16 Jan 2009; accepted 21 Jan 2009; published 9 Feb 2009

To reduce the dispersion effect, one sideband was eliminated using the proposed method. Figure 8 shows the measured RF power of transmitted signal using the SSB modulation. In contrast to DSB modulation, no notable degradation was observed. This result reveals that the proposed modulation scheme enables MMW generation and signal transmission without any power penalty caused by chromatic dispersion.

5. Conclusion

We proposed an efficient MMW up-conversion system and realized that by fabrication of integrated modulator. We introduced the periodic domain-inversion structure to achieve efficient integration of two modulators. 60GHz optical carrier signals was generated by DSB-SC modulation and then optical conversion of the IF signal to LSB (or USB) is achieved in additional SSB modulation. We also investigated the effects of modulation scheme on fiber chromatic dispersion. Measured result reveals that the proposed modulation scheme enables MMW generation and signal transmission without any power penalty caused by chromatic dispersion.

Acknowledgments

This research was supported by Ministry of Knowledge Economy (MKE), Korea as a project, "Technologies development for future home appliance."

#101333 - $15.00 USD Received 8 Sep 2008; revised 16 Jan 2009; accepted 21 Jan 2009; published 9 Feb 2009